

## Antiferromagnetic-Resonance Measurements in Europium Telluride†

J. W. BATTLES\* AND GLEN E. EVERETT

*Physics Department, University of California, Riverside, California 92502*

(Received 29 October 1969)

EuTe is a fcc antiferromagnet with ordering of the second kind. Antiferromagnetic-resonance measurements on single crystals have been performed as a function of crystallographic orientation at 1.17°K and at the frequencies 9, 18, and 24 GHz. The results show that the dominant anisotropy energy contribution is of dipolar origin and that the sublattice magnetization vectors lie in {111} planes. There is, in addition, a weak anisotropy in the (111) plane which make the  $\langle 11\bar{2} \rangle$  or equivalent directions the zero-field easy axes. The values of the dipolar and in-plane anisotropy fields are 4000 and 8 G, respectively. For this "easy-plane" behavior, the two resonant branches are nondegenerate in zero field and have the values 2 and 68 GHz. The behavior of the spin-flop transition with the magnetic field along an in-plane easy axis has been examined. The energy change associated with this transition is calculated to be  $\Delta E = [8 + (3H_f/2H_E)^2]K_2$ , where  $K_2$  is the in-plane anisotropy energy,  $H_f$  the spin-flop field, and  $H_E$  the exchange field.

### I. INTRODUCTION

EUROPIUM telluride is the fourth member of the europium chalcogenides and is the only one that is antiferromagnetic (AFM). In the paramagnetic state it has the NaCl structure. From measurements of the magnetization<sup>1</sup> and specific heat<sup>2</sup> on polycrystalline samples, the Néel temperature has been determined as being  $T_N = 9.8^\circ\text{K}$ . From early specific-heat measurements;<sup>3</sup> the experimentally determined magnetic entropy was considerably lower than what is to be expected for a simple antiferromagnet. Recent work by Passenheim<sup>4</sup> has shown that this effect is related to sample impurities. From his results on purified material, the magnetic entropy agrees with the expected theoretical result to within the experimental uncertainty. The results of powder neutron diffraction experiments<sup>5</sup> have shown that EuTe is a type-II fcc AFM, and that the spin ordering is associated with {111} crystallographic planes. Associated with the AFM transition is a lattice distortion along a  $\langle 111 \rangle$  crystallographic axis.<sup>6</sup> The corresponding set of (111) planes are the ones with which the magnetic ordering is associated. Since there are four equivalent  $\langle 111 \rangle$  directions in the paramagnetic state, the AFM state is characterized by the existence of domains, the so-called  $T$  domains,<sup>7</sup> one for each of the equivalent  $\langle 111 \rangle$  directions. While attempts to determine the lattice distortion in EuTe using x-ray tech-

niques<sup>8</sup> have not given measurable results, the domains have been observed directly optically<sup>7</sup> and indirectly from earlier antiferromagnetic-resonance (AFMR) measurements<sup>9</sup> on single crystals. In Sec. II we summarize the results of the calculation of the AFMR frequencies as a function of field and crystallographic direction for the case of a single domain. In Sec. III is a description of experimental methods followed by the results of these experiments in Sec. IV. In Sec. V we discuss the implications arising from this interpretation of our results comparing them with other experiments and suggesting additional experiments to provide a more stringent test of this model.

### II. RESONANCE EQUATIONS FOR AN EASY-PLANE ANTIFERROMAGNET

Although the uniaxial, easy-axis AFM has been extensively investigated both theoretically<sup>10</sup> and experimentally,<sup>11</sup> the alternate case of the uniaxial, easy-plane AFM has received less attention. The theoretical investigations<sup>12-14</sup> that have been performed include the anisotropy energy causing the easy-plane behavior but either do not include the additional energy giving the preferred directions in the easy plane or do not determine the resonance equations for a general crystallographic direction. A considerable amount of theoretical and experimental work has been done on the easy-plane system, but has been primarily applied to the canted

† Work supported in part by the U. S. Atomic Energy Commission, AEC Report No. UCR 34 P77-23.

\* Present address: U. S. Naval Weapons Center, Corona Laboratories, Corona, Calif. 91720.

<sup>1</sup> U. Enz *et al.*, *Phillips Res. Repts.* **17**, 451 (1962); S. van Houten, *Phys. Letters* **2**, 215 (1962); T. R. McGuire *et al.*, *Appl. Phys. Letters* **1**, 17 (1962); T. R. McGuire *et al.*, *J. Appl. Phys.* **34**, 1345 (1963).

<sup>2</sup> G. Busch *et al.*, *Phys. Letters* **11**, 9 (1964).

<sup>3</sup> G. Busch *et al.*, *Helv. Phys. Acta* **37**, 637 (1964).

<sup>4</sup> Burr C. Passenheim, Ph.D. thesis, University of California, 1969 (unpublished).

<sup>5</sup> G. Will *et al.*, *J. Phys. Chem. Solids* **24**, 1679 (1963).

<sup>6</sup> D. S. Rodbell and J. Owens, *J. Appl. Phys.* **35**, 1002 (1964). This paper is primarily concerned with the behavior of the isostructural compounds MnO and NiO and considers the physical origin of the distortion and its consequences.

<sup>7</sup> P. Wachter, *Physik Kondensierten Materie* **7**, 1 (1968).

<sup>8</sup> D. S. Rodbell, L. M. Osika, and P. E. Lawrence, *J. Appl. Phys.* **36**, 666 (1965).

<sup>9</sup> J. W. Battles and Glen E. Everett, *Solid State Commun.* **6**, 569 (1968).

<sup>10</sup> B. Lax and K. J. Button, *Microwave Ferrites and Ferromagnetics* (McGraw-Hill Book Co., New York, 1962), p. 253.

<sup>11</sup> Reference 10, p. 266.

<sup>12</sup> T. Nagamiya, K. Yosida, and R. Kubo, *Advan. Phys.* **4**, 1 (1959).

<sup>13</sup> E. A. Turov, *Physical Properties of Magnetically Ordered Crystals* (Academic Press Inc., New York, 1965), Chap. 4, pp. 55-65.

<sup>14</sup> A. I. Ahkizer, V. G. Bar'yakhtar, and S. V. Peletmiuskii, *Spin Waves* (North-Holland Publishing Co., Amsterdam, 1968), pp. 61-69.

antiferromagnetic compounds such as  $\text{MnCO}_3$ <sup>15</sup> and  $\alpha\text{-Fe}_2\text{O}_3$ <sup>16,17</sup> with the emphasis on the consequences of the canting interaction. There exist in addition the hexagonal compounds, e.g.,  $\text{CsMnF}_3$ <sup>18</sup> and  $\text{RbNiF}_3$ <sup>19</sup> which are also of the easy-plane type. The feature common to all of these systems and to  $\text{EuTe}$  is that the hard axis is an axis of threefold symmetry.

The resonance-frequency versus magnetic-field behavior common to the easy-plane system has been described by Turov in Ref. 13. It consists of two branches which are not degenerate in zero magnetic field. The high-frequency branch has a nonzero, zero-field frequency,  $\omega_{20}$ , which is related to the hard-axis anisotropy energy while the low-frequency branch also has a zero-field frequency,  $\omega_{10}$ , which is different from zero due to the in-plane anisotropy energy. Battles<sup>20</sup> has used the method of Heller,<sup>21</sup> incorporating the anisotropy energy appropriate to the type-II ordering as obtained by Keffer and O'Sullivan,<sup>22</sup> and calculated the resonant frequencies as a function of field for general crystallographic directions. Designating the coordinates of the two sublattices by the subscripts 1 and 2, this total anisotropy energy becomes

$$\mathcal{H}_A = (3K_1/8)(\gamma_1 - \gamma_2)^2 - \frac{1}{2}K_2(\sin^2 3\phi_1 + \sin^2 3\phi_2), \quad (1)$$

where  $\gamma_i = \cos\theta_i$  is the appropriate direction cosine with respect to the  $z$ , or hard axis. (The  $z$  axis corresponds to a (111) crystallographic axis.) The angle  $\phi_j$  is the angle in the plane between an in-plane hard axis, the  $x$  axis, and the sublattice magnetization vector. The term in  $K_1$  is the dipolar anisotropy as calculated by Kaplan<sup>23</sup> and the term in  $K_2$  is the phenomenological in-plane anisotropy energy. The higher-order anisotropy contributions allowed by symmetry have been neglected. We note that the existence of the  $S$  domains as described in the introduction requires  $K_2 \neq 0$ . In the presence of an external magnetic field the total energy of the system will contain the Zeeman energy in addition to the exchange and anisotropy energies. Representing this total energy by  $\mathcal{H}$  and the variables by  $\eta_i, \boldsymbol{\eta} = (\theta_1, \theta_2, \phi_1, \phi_2)$ , the equilibrium condition for the system is determined

<sup>15</sup> M. Date, J. Phys. Soc. Japan 15, 2251 (1960); E. A. Turov and N. G. Guseinov, Zh. Eksperim. i Teor. Fiz. 38, 1326 (1960) [English transl.: Soviet Phys.—JETP 11, 955 (1960)]; H. J. Fink and D. Shaltiel, Phys. Rev. 130, 627 (1963); A. S. Borovik-Romanov, N. M. Kreines, and L. A. Prozorova, Zh. Eksperim. i Teor. Fiz. 45, 64 (1963) [English transl.: Soviet Phys.—JETP 18, 46 (1964)].

<sup>16</sup> P. Pincus, Phys. Rev. Letters, 5, 13 (1960).

<sup>17</sup> P. J. Besser, A. H. Morrish, and C. W. Searle, Phys. Rev. 153, 632 (1967).

<sup>18</sup> K. Lee, A. M. Portis, and G. L. Witt, Phys. Rev. 132, 144 (1963).

<sup>19</sup> E. I. Golovenchits, V. A. Sanina, and A. G. Gurevich, Fiz. Tverd. Tela 10, 2956 (1968) [English transl.: Soviet Phys.—Solid State 10, 2334 (1969)].

<sup>20</sup> J. W. Battles, Ph.D. dissertation, University of California, Riverside, 1969 (unpublished).

<sup>21</sup> G. S. Heller, Lincoln Laboratory Quarterly Progress Report, April, 1961 (unpublished) (also summarized in Ref. 10, Appendix 6-2, p. 292).

<sup>22</sup> F. Keffer and W. O'Sullivan, Phys. Rev. 108, 637 (1957).

<sup>23</sup> J. I. Kaplan, J. Chem. Phys. 22, 1709 (1954).

by the solution of the following set of equations:

$$\partial\mathcal{H}/\partial\eta_i = 0, \quad i = 1, \dots, 4. \quad (2)$$

The resonance frequencies are now determined in the small-signal approximation by the solutions of the equation

$$\det \left\{ \frac{\partial^2 \mathcal{H}}{\partial \eta_i \partial \eta_j} + \frac{j\omega M}{\gamma} \sin \eta_i (\delta_{i+2,j} - \delta_{i,j+2}) \right\} = 0. \quad (3)$$

This equation is quadratic in  $\omega^2$  and has two independent solutions  $\omega_2$  and  $\omega_1$  ( $\omega_2 > \omega_1$ ) which is referred to as the high- and low-frequency branches, respectively. We now summarize the results obtained by Battles<sup>20</sup> for the magnetic field in a general direction but lying in a principle crystallographic plane.

### $H$ in (111) Plane

For  $H$  lying in the (111) plane and making an angle  $\alpha$  with respect to the  $x$  axis (the in-plane hard axis), the Zeeman energy becomes

$$\mathcal{H}_Z = -HM[\cos\alpha(\sin\theta_1\cos\phi_1 + \sin\theta_2\cos\phi_2) + \sin\alpha(\sin\theta_1\sin\phi_2 + \sin\theta_2\sin\phi_1)]. \quad (4)$$

For convenience we define the following quantities:

$$H_a = 9K_2/M, \quad H_A = \frac{3}{4}K_1/M, \quad H_E = \lambda M,$$

where  $H_a, H_A$ , and  $H_E$  are called the in-plane, the out-of-plane or dipolar, and the exchange or molecular fields, respectively. In making the approximations that follow, we assume  $H_a \ll H_A \ll H_E$ . In addition, it is necessary to distinguish between the normal and the spin-flopped states, determined by whether or not the field is less or greater than the spin-flop field,  $H_f$ . An expression for the spin-flop field has been obtained by Keffer and O'Sullivan.<sup>22</sup> Their result is in agreement with ours but we initially found their derivation and its consequences rather obscure. [Agreement is obtained with their  $H_a'$ , Eq. (47), with the in-plane anisotropy as given by Eq. (40).] We summarize a calculation of  $H_f$  which we feel is more clear.

The total energy of the system is given by

$$\begin{aligned} \mathcal{H} = & \lambda M^2[\sin\theta_1 \sin\theta_2 \cos(\phi_1 - \phi_2) + \cos\theta_1 \cos\theta_2] \\ & - HM[\cos(\alpha - \phi_1) + \cos(\alpha - \phi_2)] \\ & - \frac{3}{8}K_1[2 - (\cos\theta_1 - \cos\theta_2)^2] \\ & - \frac{1}{2}K_2[\sin^2 3\phi_1 + \sin^2 3\phi_2]. \end{aligned} \quad (5)$$

The equilibrium values of  $\theta_1$  and  $\theta_2$  are  $\theta_1 = \theta_2 = \frac{1}{2}\pi$ . Defining the new angles  $\phi_0$  and  $\eta$  by

$$\phi_1 = \phi_0 - \eta \quad \text{and} \quad \phi_2 = \pi + \phi_0 + \eta$$

and inserting into Eq. (5) results in the following expression for  $\mathcal{H}$ :

$$\begin{aligned} \mathcal{H} = & \mathcal{H}_0 + 2\lambda M^2 \sin\eta[\sin\eta + (H/\lambda M)\sin(\alpha - \phi_0)] \\ & + \frac{1}{2}K_2[1 + \cos 6\phi_0 \cos 6\eta], \end{aligned} \quad (6)$$

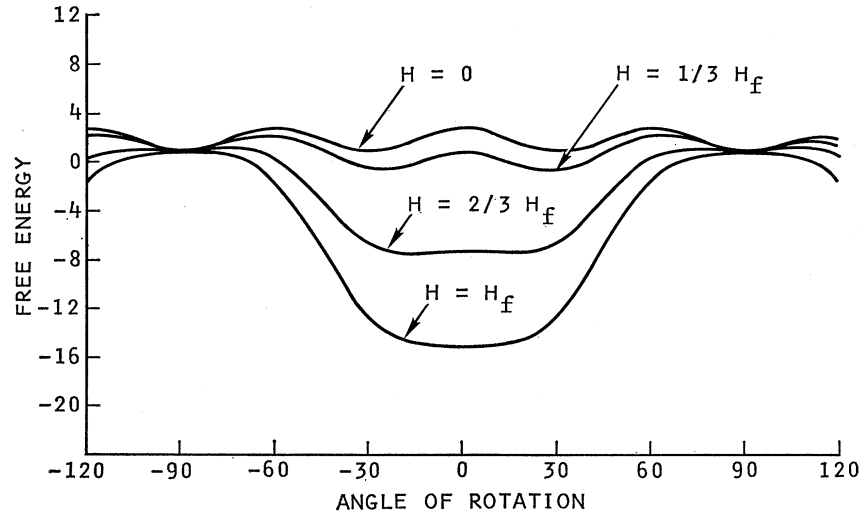


FIG. 1. Magnetic energy as a function of the angle  $\phi_0$  between the sublattice magnetization vector and the  $\hat{x}$  (in-plane hard-direction) axis for the applied field parallel to the  $\hat{y}$  (in-plane easy-direction) axis.

where

$$3\mathcal{C}_0 = -\lambda M^2 - \frac{3}{4}K_1 - K_2.$$

The new equilibrium conditions,  $\partial\mathcal{C}/\partial\eta=0$  and  $\partial\mathcal{C}/\partial\phi_0=0$ , determine the values of  $\phi_0$  and  $\eta$ . In zero magnetic field these are  $\phi_0=\frac{1}{2}\pi$  and  $\eta=0$ . For EuTe,  $H_a/6H_E \sim 4 \times 10^{-5}$  and can be neglected for  $H \geq H_a$ . Using this approximation and imposing the condition  $H/2H_E \ll 1$ , we can treat  $\eta$  as a small quantity and obtain the following expression:

$$\eta = \frac{-H}{2H_E} \frac{\sin(\alpha - \phi_0)}{[1 + (H/2H_E) \cos(\alpha - \phi_0)]}. \quad (7)$$

Using this expression,  $\phi_0$  can be calculated and is given by

$$H^2 \sin 2(\alpha - \phi_0) = \frac{2}{3} H_a H_E \sin 6\phi_0. \quad (8)$$

These expressions have been used in calculating the resonance equations.

For the case of the magnetic field along a hard axis,  $\alpha=0$ ,  $\phi_0=\frac{1}{2}\pi$ , and  $\sin\eta=H/2H_E$ . A calculation of the "in-plane perpendicular susceptibility" gives the result

$$\chi_1 = (1/\lambda)(1 - H_a/2H_E). \quad (9)$$

The other case of interest is when  $\alpha=\frac{1}{2}\pi$ ,  $H$  along an easy axis. To display the behavior of the system, we have used a computer to numerically solve for  $\eta$  as a function of  $\phi_0$  and determined the energy as a function of  $\phi_0$  for different magnetic fields as shown in Fig. 1. In zero magnetic field the assumed direction of the sublattice magnetization vectors is  $\pm 90^\circ$  and corresponds to a minimum energy. For  $0 < H < H_f$ , these positions become metastable and are confined to this position by the "anisotropy hump." At  $H=H_f$ , this hump ceases to exist and the system switches to the spin-flopped position,  $\phi_0=0$ . If we use one of the exact equilibrium conditions to express  $\eta$  as a function of  $\phi_0$ , the spin-flop

field is determined by the field at which

$$\left. \frac{\partial^2 \mathcal{C}}{\partial \phi_0^2} \right|_{\phi_0=\pi/2, \eta=0} = 0.$$

We have determined this derivative making no approximations and determine the spin-flop field to be

$$H_f^2 = 2H_a H_E (1 + H_a/2H_E) \cong 2H_a H_E. \quad (10)$$

Using Eq. (9) and the approximation  $(1/\chi_1) \cong \lambda(1 + H_a/2H_E)$ , the spin-flop field takes the form

$$H_f \cong (18K_2/\chi_1)^{1/2}. \quad (11)$$

Associated with the spin-flop is a discontinuous change in the magnetic energy given by

$$\Delta E = -[8 + (3H_f/2H_E)^2]K_2. \quad (12)$$

Heating effects in an alternating magnetic field (2 kOe) have been reported by Busch *et al.*<sup>24</sup> in powder samples of EuTe which may be a reflection of this energy change. Their paper does not, however, give sufficient detail for a definite conclusion. We note, finally, that these expressions have been obtained in the molecular-field approximation for  $T=0^\circ\text{K}$  and in particular have neglected any effects due to spin-wave excitations. For a thermally isolated single  $S$ -domain sample, this corresponds to a step temperature rise in the sample.

#### Case 1: $H < H_f$

Using Eq. (2) to determine the equilibrium values of the angles ( $\theta_1, \theta_2, \phi_1, \phi_2$ ) to first order in the applied magnetic field and subject to the condition  $H/H_E \ll 1$ , we have determined the resonant frequencies to be

$$(\omega_1/\gamma)^2 = 2H_a H_E + H^2 \cos 2\alpha (1 - H^2 \sin^2 \alpha / H_a H_E) - H^2 \cos^2 \alpha (H^2 \sin^2 \alpha / 4H_E^2) \quad (13)$$

<sup>24</sup> G. Busch *et al.*, Phys. Letters 9, 7 (1964).

and

$$\left(\frac{\omega_2}{\gamma}\right)^2 = 4H_A H_E + 2H_a H_A - H^2 \cos^2 \alpha \left[ \frac{H_A}{H_E} - \frac{H^2 \sin^2 \alpha}{H_A H_E} + \frac{H^2 \sin^2 \alpha}{4H_E^2} \right] + 3H^2 \sin^2 \alpha \left[ 1 - \frac{H^2 \sin^2 \alpha}{3H_A H_E} \right]. \quad (14)$$

For the magnetic field applied along the hard direction,  $\alpha = 0$ , Eqs. (13) and (14) become

$$(\omega_1/\gamma)^2 = H^2 + 2H_a H_E \quad (15)$$

and

$$(\omega_2/\gamma)^2 = 4H_A H_E + 2H_a H_A - (H_A/H_E)H^2. \quad (16)$$

For this orientation, there is no spin-flop transition. These equations are valid for all fields subject to the approximation that  $(H/H_E) \ll 1$ . This dependence on field is shown in Fig. 2. For the applied field along the easy axis,  $\alpha = \frac{1}{2}\pi$ , the resonance equations, to first order in  $H/H_E$ , become

$$(\omega_1/\gamma)^2 = 2H_a H_E - H^2 \quad (17)$$

and

$$(\omega_2/\gamma)^2 = 4H_A H_E + 2H_a H_A + 3H^2. \quad (18)$$

The resonant frequency  $\omega_1$  goes to zero at

$$H = (2H_a H_E)^{1/2},$$

the spin-flop field.

**Case 2:  $H > H_f$**

For the spin-flopped mode, it is more convenient to introduce the angles  $\delta_1$  and  $\delta_2$  defined by

$$\phi_1 = \frac{1}{2}\pi + \alpha - \delta_1 \quad \text{and} \quad \phi_2 = \frac{3}{2}\pi + \alpha + \delta_2.$$

Determining these small quantities to first order in  $(H/H_E)$  and substituting into the resonance equation gives

$$(\omega_1/\gamma)^2 = H^2 + 2H_a H_E \cos 6\alpha \quad (19)$$

and

$$(\omega_2/\gamma)^2 = 4H_A H_E + 2H_a H_E \cos 6\alpha - (H_A/H_E)H^2. \quad (20)$$

These equations are subject to the restriction  $H/H_E \ll 1$ . For the case of  $\mathbf{H}$  along the easy axis,  $\alpha = \frac{1}{2}\pi$ , these become

$$(\omega_1/\gamma)^2 = H^2 - 2H_a H_E \quad (21)$$

and

$$(\omega_2/\gamma)^2 = 4H_A H_E - 2H_a H_E - (H_A/H_E)H^2 \quad (22)$$

The results for  $H < H_f$  together with  $H > H_f$  are shown in Fig. 3. The upper branch has a discontinuous change at  $H = H_f$ , but otherwise depends only weakly on the

FIG. 2. Field dependence of the resonant frequencies for the special case of the applied field parallel to an in-plane hard axis. The dashed line represents the limit of the in-plane anisotropy energy,  $H_a$ , equal to zero.

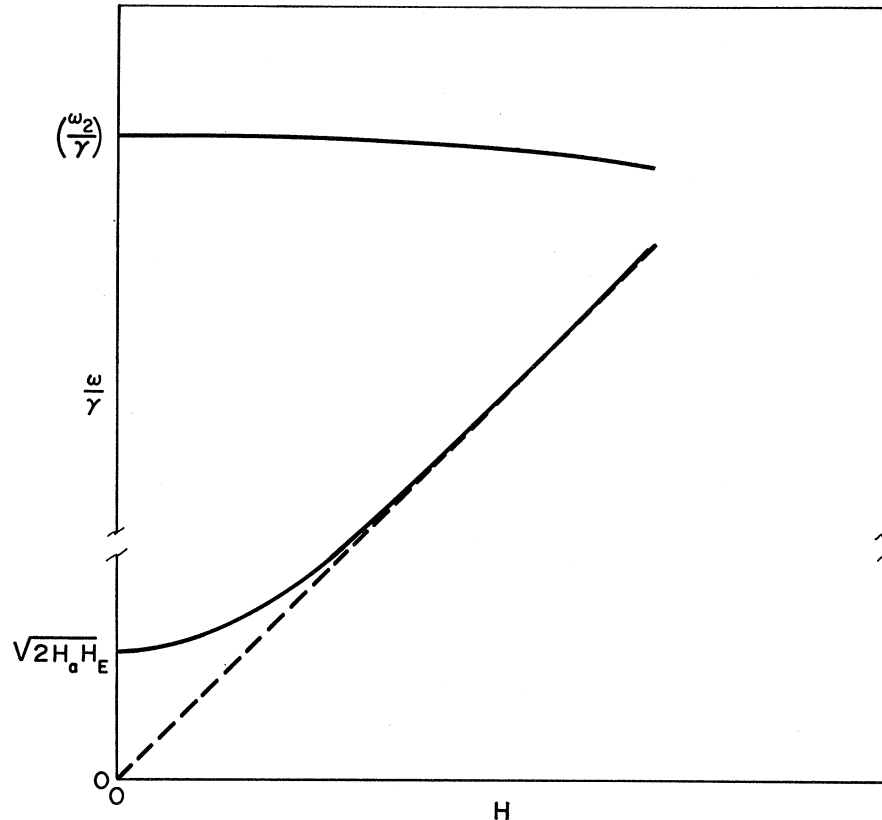
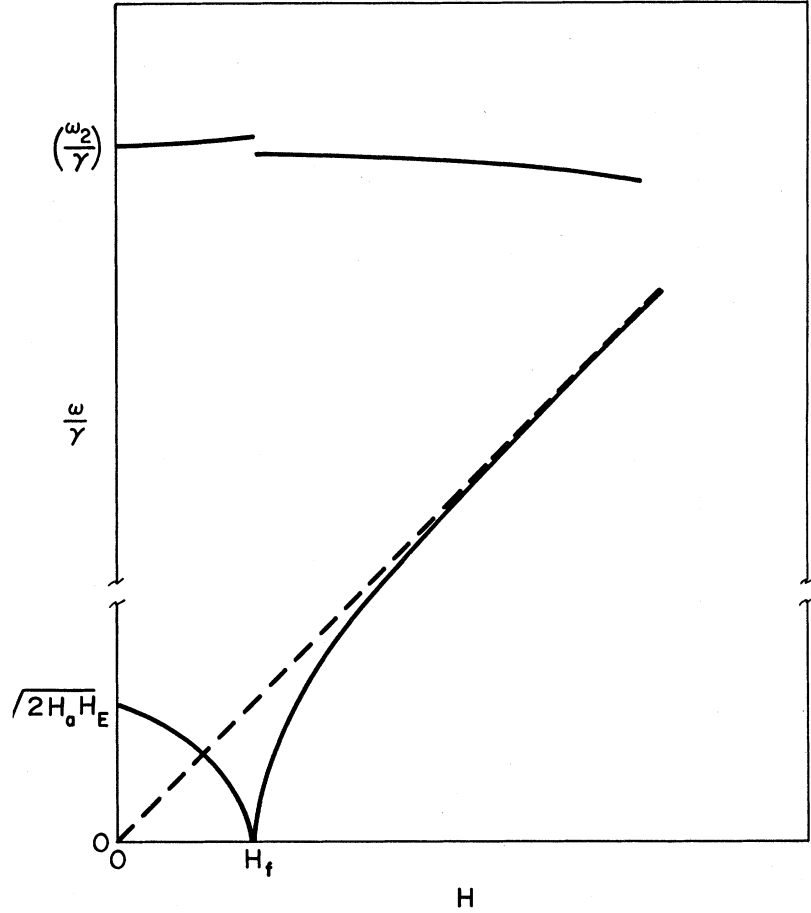


FIG. 3. Field dependence of the resonant frequencies for the special case of the applied field parallel to an in-plane easy axis.  $H_f$  is the spin-flop field, Eq. (10). The resonant frequency of the upper branch changes discontinuously at  $H=H_f$ . The difference in the squares of this frequency is  $\Delta(\omega_2/\gamma)^2 = 6H_a(H_E+H_A) \approx 3H_f^2$ . The dashed line represents the limiting behavior of the low-frequency branch when  $H_a=0$



field. The slope of  $\omega_2$  above  $H_f$  must become positive at high fields. This reflects the neglect of terms like  $(H/H_E)^4$  in this derivation. The results, Eq. (19), are identical to those obtained for the hexagonal easy-plane AFM,  $\text{CsMnF}_3$ <sup>18</sup> as well as for  $\alpha\text{-Fe}_2\text{O}_3$  where the canting interaction is weak. The  $\cos 6\alpha$  angular dependence in the spin-flopped state is not present for  $H < H_f$  since the sublattice magnetization vectors remain fixed, essentially, to the easy axes.

#### $H$ not in a (111) Plane

When the applied field does not lie in the (111) plane, the resonance equations are obtained by this same procedure. To illustrate the results obtained, we consider the case where the applied field lies in the  $y$ - $z$  plane, making an angle  $\beta$  with the  $z$  axis. The result is two branches as before with two cases depending on whether or not one is above or below the spin-flop field. For the spin-flopped state the resonant frequencies are given by

$$(\omega_1/\gamma)^2 = H^2[\sin^2\beta - (H^2/16H_A H_E)\sin^2 2\beta] - 2H_a H_E \quad (23)$$

and

$$(\omega_2/\gamma)^2 = 4H_A H_E - 2H_a H_A - (H_A/H_E)H^2 + H^2 \cos^2\beta [1 - (H^2/16H_E^2)\cos^2\beta + (H^2/4H_A H_E)\sin^2\beta]. \quad (24)$$

When the applied field is parallel to the (111) direction, a hard axis,  $\beta=0$  and Eqs. (23) and (24) reduce to

$$(\omega_1/\gamma)^2 = 2H_E H_a - (H_a/2H_E)H^2 \quad (25)$$

and

$$(\omega_2/\gamma)^2 = 4H_A H_E + 2H_A H_a + H^2 \times [1 - 2H_A/H_E - H^2/4H_E^2]. \quad (26)$$

A plot of Eqs. (25) and (26) is given in Fig. 4. In this case  $\omega_1$  is almost field-independent. The high-frequency mode  $\omega_2$  shows the usual increase with increasing field. The presence of the negative term in  $(H/2H_E)^2$  indicates that the rise is less rapid than  $H^2$  but does not provide the possibility of a decrease because of the approximation made in this calculation. It is of interest to observe that in the limit of  $H_a \approx 0$  and low fields, Eq. (23) reduces to

$$\omega_1/\gamma = H \sin\beta, \quad (27)$$

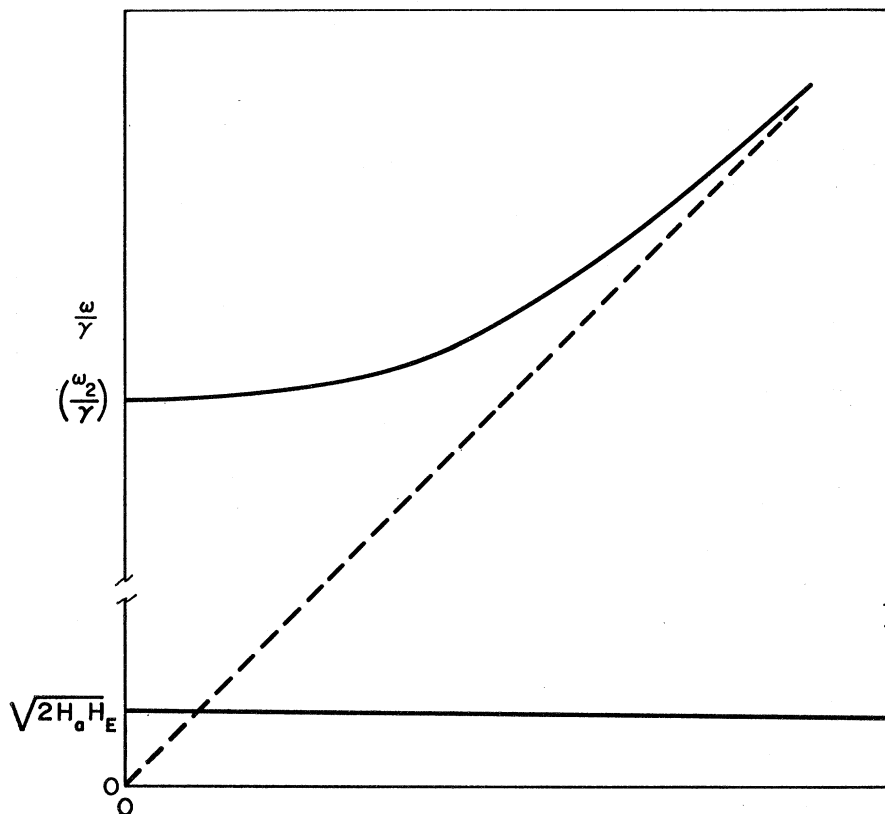


FIG. 4. Field dependence of the resonance frequencies for the special case of the applied field perpendicular to the easy plane. The low-frequency branch is nearly field independent. The dashed line has been included to indicate the limiting behavior. When  $H_a=0$ , the low-frequency branch is zero independent of field.

the result initially determined by Pincus<sup>16</sup> neglecting the in-plane anisotropy energy, and by Turov and Guseinov<sup>15</sup> if we set  $q$  in their Eq. (5) equal to zero. This simple behavior can be described by observing that the field for resonance at a particular angle is that required to give a constant value of the projection,  $(\omega_0/\gamma)$ , on the easy plane. With this approximation the system is always in the spin-flopped state.

To summarize the results of this section, we have presented results for the field and angular dependence of the two resonant-frequency branches below and above the spin-flop field. The results have, in each case, been extended to higher order in  $H/2H_E$  than have been previously given in the literature. Anticipating our experimental results, we observe that these additional terms become particularly important for the magnetic field making a large angle with the easy plane.

### III. EXPERIMENTAL PROCEDURE

The compound EuTe was prepared by the direct reaction of the elements. The material was purified by fractional distillation which also yielded small but usable single crystals. Single crystals were ground into spheres, the surface polished, and annealed for 12 h at 900°C. The samples obtained were between 0.1 and 0.2 mm in diam. Using an x-ray precession camera, the samples were oriented and mounted such that the static magnetic field would lie in either a (111) or (110) plane.

The microwave spectrometer used was of a conventional design.<sup>25</sup> For some measurements at 24 GHz, a homodyne detection system with automatic phase control<sup>26</sup> was used to improve sensitivity. Figure 5 shows a cutaway of the cavity section of the sample holder, the sample being rotated around the axis of the waveguide. The vacuum-tight can, provided to permit temperature variations above 4.2°K, served to exclude liquid helium from the cavity and waveguide. This reduces the overall noise in the system. To maintain thermal contact with the sample, the can was filled with helium gas to a pressure of about 300  $\mu$ .

For the measurements at 18 and 24 GHz, a common sample holder was used. The temperature of this system was 1.17°K. The measurements at 9 GHz were with a different Dewar system and were taken at 1.35°K.

### IV. EXPERIMENTAL RESULTS

Data taken for the magnetic field rotated in {110} and {111} planes is shown in Figs. 6–8. The data shown in Fig. 6 is for the magnetic field in a (111) plane taken at 9 GHz. The data is characterized by four branches, one being associated with each of the possible  $T$  domains. For one of these, branch  $B$ , the magnetic field lies in the plane of the spins for this domain. The re-

<sup>25</sup> Reference 10, Chap. 10.

<sup>26</sup> H. C. Praddaude, Rev. Sci. Instr. **38**, 339 (1967).

maining branches are associated with the other three domains. For perfect alignment of the crystal, these branches should be identical but separated by 120°. Each branch having a 2θ angular dependence gives the observed result of a maximum in the field for resonance every 60°. The maxima not being at the same field value is attributed to a small misorientation of the sample.

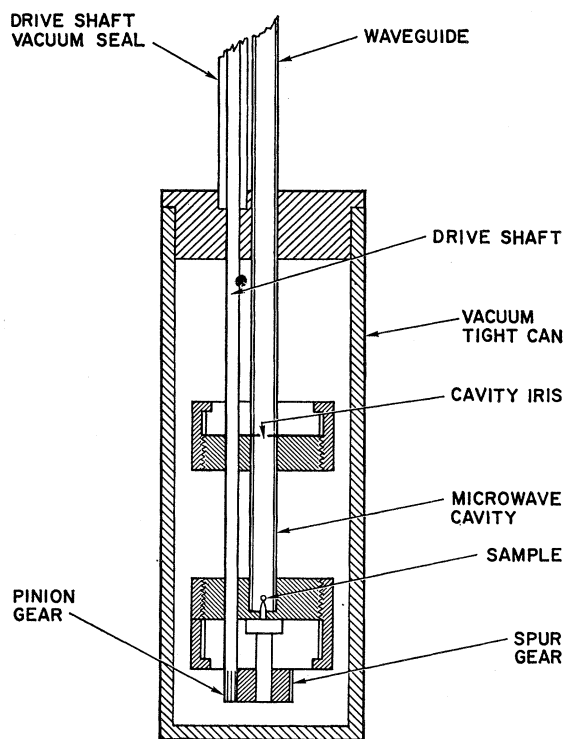


FIG. 5. Cutaway drawing of the low-temperature portion of the sample holder. Details of thermometers, heater, and pumping lines have been omitted for clarity.

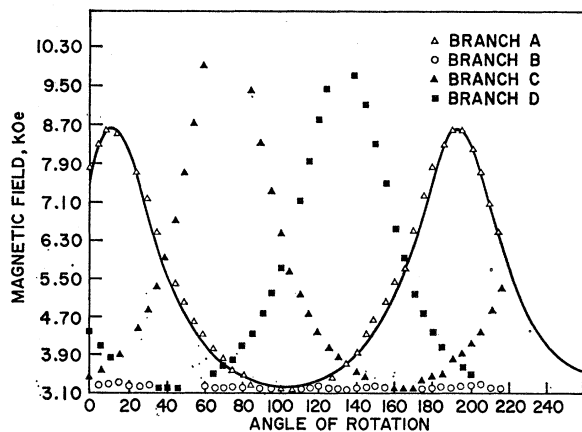


FIG. 6. Magnetic field for resonance as a function of crystallographic direction at the constant frequency 9 GHz. The sample is a single crystal with the magnetic field lying in a (111) plane. The four branches shown arise from the four different possible types of domains as discussed in the text. The solid curve is the result of fitting to Eq. (29) with the appropriate value of α.

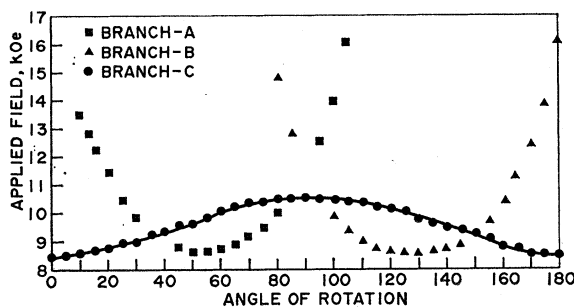


FIG. 7. Magnetic field for resonance as a function of crystallographic direction at the constant frequency 24 GHz. The sample is a single crystal with the magnetic lying in a (110) plane. The solid curve is the result of fitting branch C to Eq. (29).

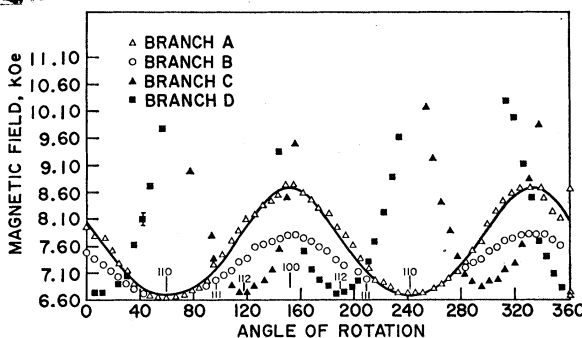


FIG. 8. Magnetic field for resonance as a function of crystallographic direction at the constant frequency 18 GHz. The sample is a single crystal with a slight misorientation such that the magnetic field lies nearly in a (110) plane. The branches A and B are distinct owing to the misorientation and correspond to branch C, Fig. 7. The solid curve is the result of fitting this branch to Eq. (29).

From the results obtained for rotations out of the easy plane, Eq. (23), the field for resonance as a function of angle can be rewritten as

$$H(\beta) = H_0 / \sin \beta, \tag{28}$$

where  $H_0^2 = (\omega_0/\gamma)^2 + 2H_a H_E$  and  $\omega_0$  is the fixed frequency at which the measurements are being made. [The term in  $\sin^2 \beta$ , Eq. (23), has been neglected.] The solid curve drawn through the points, branch B in Fig. 6, has been calculated and represents the projection of  $H$  into the easy plane of this  $T$  domain being equal to  $H_0$ . The angle between this easy plane and the plane in which the magnetic field is being rotated is  $\alpha$  and the equation for the resonant field as a function of angle becomes

$$H(\beta') = H_0 [1 - \cos^2 \beta' \cos^2 \alpha]^{-1/2}. \tag{29}$$

The quantity  $H_0$  being different from  $(\omega_0/\gamma)$  provides a determination of  $2H_a H_E$ . We have made use of the fact  $H_0 > (\omega_0/\gamma)$  and the frequency dependence to identify these branches as being those of the low-frequency spin-flopped mode. The very good fit of Eq. (29) to this branch without the higher-order terms included is

an indication of the fact that for these fields and angles, the sublattice magnetization vectors are effectively not being pulled out of the easy plane.

For the case of the magnetic field in a  $\{110\}$  plane, we would expect four branches as before but with two of them being degenerate. The results shown in Fig. 7 were obtained with the magnetic field rotated in a  $\{110\}$  plane at 24 GHz. The branch labeled *C* is the result of the two branches that are equivalent. The solid curve through these points is given by Eq. (28) with the appropriate value of  $\alpha$ . The branches *A* and *B* are the other two branches and represent rotations from an equivalent  $\langle 11\bar{2} \rangle$  direction in the plane to the  $\langle 111 \rangle$  or hard direction. The very rapid increase of the field for resonance as we approach a  $\langle 111 \rangle$  direction is what is expected from the simplified result, Eq. (27).

We have included the results of a set of measurements at 18 GHz for a sample rotated in a  $\{110\}$  plane but which was unintentionally misoriented. The result is to remove the degeneracy of the two branches labeled *C* in Fig. 7 and give the two separate branches *A* and *B* shown in Fig. 8.

The data associated with branch *A* in Fig. 7 together with the results of similar measurements on two additional samples have been plotted on one curve appropriate to this branch in Fig. 9. The solid curve is the result of fitting the results from just one sample to the theoretical equation, Eq. (23). The fit to all of the data

is very good particularly since the results of only one sample were used to determine the curve. It is to be noted that both the  $\sin^2\beta$  and  $\sin^22\beta$  terms of Eq. (23) were required to obtain this agreement between experiment and theory. The dashed curve, Fig. 9, is the result of using Eq. (28) with  $H_0$  determined by the minimum resonant field. The deviation from this simple equation reflects the importance of including the amount by which the sublattice magnetization vectors are pulled out of the easy plane for these angles and fields. Data to 24 kOe represented the limit of our available magnetic field. It would be of interest to extend these measurements to higher fields for testing the range of usefulness of the resonance equations obtained. How successful this would be is not clear as the linewidth is also increasing as  $1/\sin\beta$ .

Our interpretation of these results is that they correspond to the low-frequency branch (branches because of domains) of a spin-flopped easy-plane AFM. The easy axis in the plane has been determined as a  $\langle 11\bar{2} \rangle$  or equivalent direction. The alternate possibilities can be ruled out using Kaplan's<sup>23</sup> results to calculate  $H_A$ . The resultant zero-field frequency is  $\sim 100$  GHz based on these estimates and cannot be observed at the frequencies we used. In fitting the data shown in Fig. 9, the ratios  $H_a/H_E$  and  $H_A/H_E$  were determined. To calculate  $H_E$ , we have used the expressions

$$H_E = \lambda M \quad \text{and} \quad \lambda = (12/g^2\mu_B^2N)(J_1 + J_2)$$

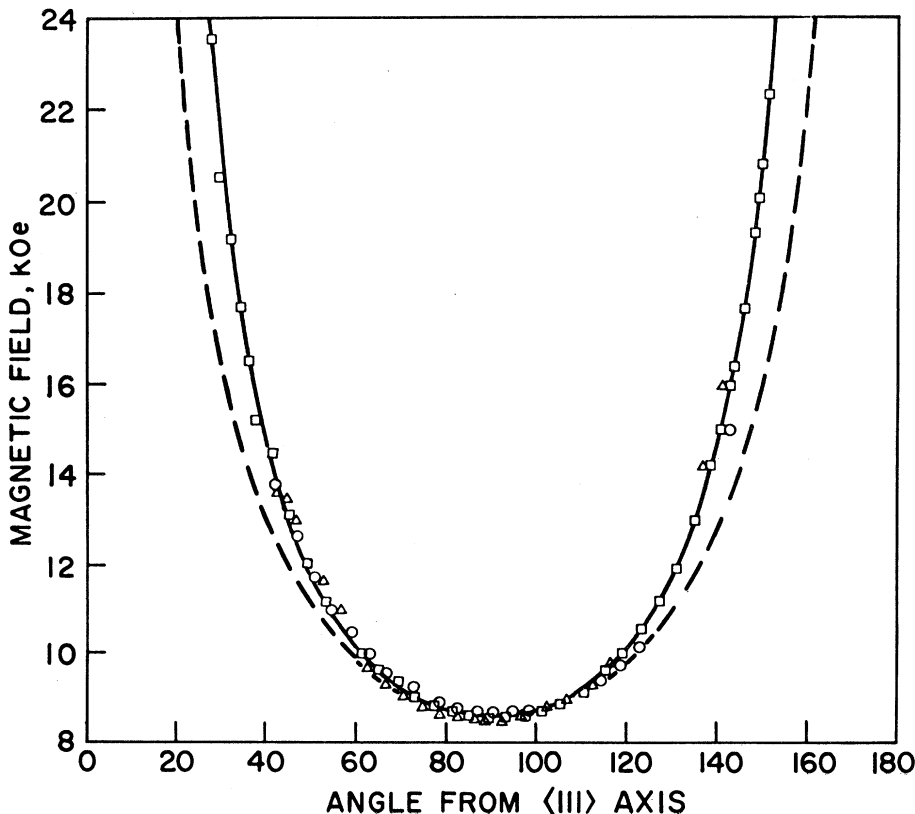


FIG. 9. Magnetic field for resonance of one branch in a  $\{110\}$  plane, as a function of crystallographic direction. The other branches, Figs. 6 and 7 have been omitted for clarity. The solid curve is the theoretical fit to the data using Eq. (23) and those points designated by squares. The other data points are from other samples in this orientation. The dashed curve is the  $1/\sin\beta$  dependence obtained Eq. (27), when the second-order effects are neglected.



together with the experimental results for  $J_1$  and  $J_2$  determined by Passenheim.<sup>4</sup> The value,  $H_E=37\pm 3$  kOe, is consistent with the value obtained from a calculation using the Néel and paramagnetic Curie temperatures. The resulting numerical quantities are as follows:

$$\begin{aligned} H_a &= (8\pm 4) \text{ Oe}, \\ H_A &= 4.0\pm 0.4 \text{ kOe}, \\ H_f &= 770\pm 200 \text{ Oe}. \end{aligned}$$

The calculated zero-field resonant frequencies are  $\omega_{10}=2$  GHz and  $\omega_{20}=68$  GHz.

## V. DISCUSSION AND CONCLUSIONS

We have treated the anisotropy energy denoted by  $K_1$  as being of dipolar origin and thus causing the easy-plane ordering. Using the relation  $K_1=\frac{4}{3}MH_A$  defined earlier and our experimental result, we obtain  $K_1=2.4\times 10^6$  erg/cm<sup>3</sup>. This result is about 20% lower than what is calculated using Kaplan's<sup>23</sup> expression. A similar discrepancy has been observed to exist by Lines and Jones for MnO<sup>27</sup> and MnS<sup>28</sup> as determined from NMR data. An attempt to interpret this difference as being caused by pseudo-dipolar effects can be discounted based on results for the high-temperature paramagnetic resonance linewidth. These results agree well with dipolar broadening theory and the classical dipolar coupling constant.<sup>29</sup>

The physical origin of the in-plane anisotropy energy,  $H_a$ , is not unambiguously determined. It could, in principle, be due to the quadrupolar terms considered by Kaplan. From the work on the anisotropy constants in the ferromagnetic europium compounds,<sup>30-32</sup> it has been determined that dipolar and higher-order terms do not contribute. The anisotropy appears to be due to the single-ion mechanism proposed by Wolff,<sup>33</sup> arising purely from crystal-field effects. The magnitude of  $H_a$  should

<sup>27</sup> M. E. Lines and E. D. Jones, Phys. Rev. **139**, A1313 (1965).

<sup>28</sup> M. E. Lines and E. D. Jones, Phys. Rev. **141**, 525 (1966).

<sup>29</sup> S. von Molnar and A. W. Lawson, Phys. Rev. **139**, A1598 (1965).

<sup>30</sup> N. Miyata and B. E. Argyle, Phys. Rev. **157**, 448 (1967).

<sup>31</sup> M. C. Franzblau, Glen E. Everett, and A. W. Lawson, Phys. Rev. **164**, 716 (1967).

<sup>32</sup> R. F. Brown, A. W. Lawson, and Glen E. Everett, Phys. Rev. **172**, 559 (1968).

<sup>33</sup> W. P. Wolf, Phys. Rev. **108**, 1152 (1957).

be compared with the values of  $K_2$  determined for these compounds recognizing that  $K_2$  as used here is defined relative to a {111} plane while the other determinations are referred to the cube edges. A transformation from the cube-edges system  $K_2'$  to the {111}-plane  $K_2$  gives the approximate relation,  $K_2\simeq K_2'/50$ . The value of  $K_2$  for EuTe is roughly a factor of 2-3 larger than the values obtained for EuO<sup>34</sup> and EuSe.<sup>32,35</sup>

A final comment is appropriate. The calculations of Pearson<sup>36</sup> have shown that the distortion accompanying the AFM state has a very pronounced effect on the anisotropy constants. The demonstrated existence of  $T$  domains in this material would only further enhance these effects. This is indirectly supported by the anomalous behavior of the temperature dependence of the anisotropy constants in EuSe.<sup>35</sup> Experiments on single-domain samples would be very useful to determine the role of domain-boundary stress effects both on  $K_1$  and on  $K_2$ .

We can summarize our results as being well described by a model for the magnetic ordering in EuTe as being of the easy-plane type. The multiple branches observed in the AFMR results are explained by the existence of domains. The observation of domains in EuTe by optical techniques<sup>7</sup> is very strong support for this model. Experiments on single-crystal samples that have been forced into a single domain by cooling in either a strong temperature gradient or under a small uniaxial stress, would be expected to exhibit just one resonant branch each for  $\omega_1$  and  $\omega_2$ . We are presently engaged in extending these measurements to lower frequencies to examine the behavior of  $\omega_1$  in the region around the spin-flop field and will attempt to do so on single-domain samples.

## ACKNOWLEDGMENTS

We would like to acknowledge many helpful discussions with Professor A. W. Lawson during the course of this investigation. We would also like to acknowledge the cooperation of Fred Essig of the U. S. Naval Weapons Center, Corona Laboratories, particularly while the manuscript was being prepared.

<sup>34</sup> Richard S. Hughes (private communication).

<sup>35</sup> Ray C. Jones (private communication).

<sup>36</sup> J. J. Pearson, Phys. Rev. **121**, 695 (1961).